School of Natural Sciences and Mathematics

Broadband Transient Absorption Study of Photoexcitations in Lead Halide Perovskites: Towards a Multiband Picture

Citation:

Anand, B., S. Sampat, E. O. Danilov, W. Peng, et al. 2016. "Broadband transient absorption study of photoexcitations in lead halide perovskites: Towards a multiband picture." Physical Review B - Condensed Matter and Materials Physics 93(16), doi:10.1103/PhysRevB.93.161205

SUPPLEMENTARY INFORMATION for A broadband transient absorption study of photoexcitations in lead halide perovskites: towards a multi-band picture

Benoy Anand,[1] Siddharth Sampat,[1] Evgeny O. Danilov,[2] Weina Peng,[3] Sara M. Rupich,[3] Yves J. Chabal,[3] Yuri N. Gartstein,[1] and Anton V. Malko[1]

[1]*Department of Physics, The University of Texas at Dallas, Richardson, Texas 75080, USA*

[2]*Department of Chemistry, North Carolina State University, Raleigh, NC 27695, USA*

[3]*Department of Material Science and Engineering, The University of Texas at Dallas, Richardson, Texas 75080, USA*

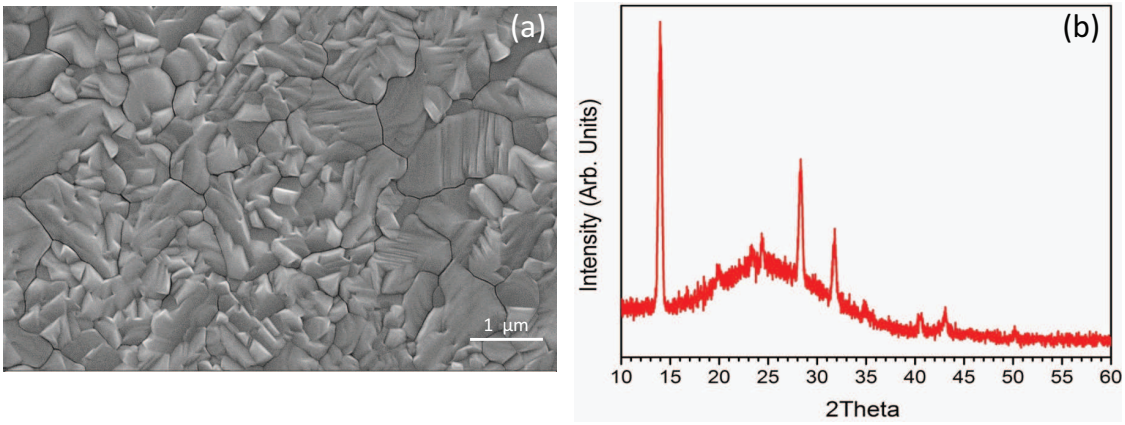

FIG. S1. (a) SEM image of $CH_3NH_3PbI_3$ films with an average grain size of 1μm. Presence of additional additional facets on the grain surface is visible. (b) XRD spectrum of the sample shows no evidence of the remaining PbI_2 phase (12.6°peak), indicating complete conversion and no structural degradation at the annealing temperature (150°C). Preferential growth is along the (110) direction, with 14.0°(110), 28.3°(220) and 31.8°(310) being the most prominent diffraction peaks.

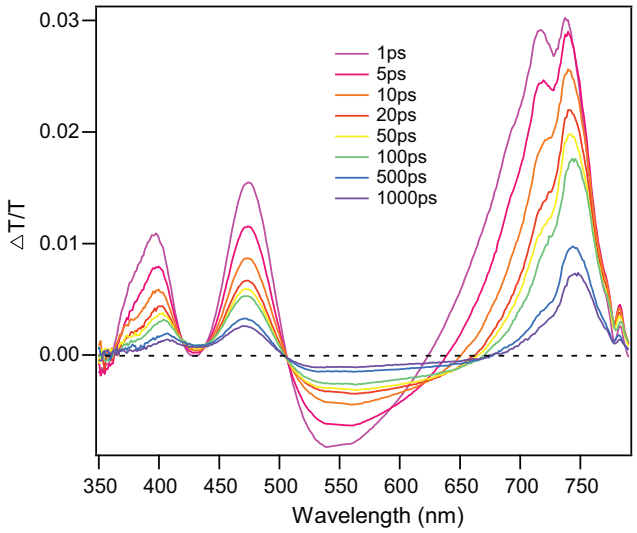

FIG. S2. UV-Vis TA spectra measured with 550 nm photoexcitation. As in the case of 303 nm pump, all the three PB peaks are simultaneously present suggesting that bleach features at spectrally different regimes are primarily due to band-edge excitations. PB1 peak shows spectral modulation due to the fluctuations of the weak WLC probe at those wavelengths.

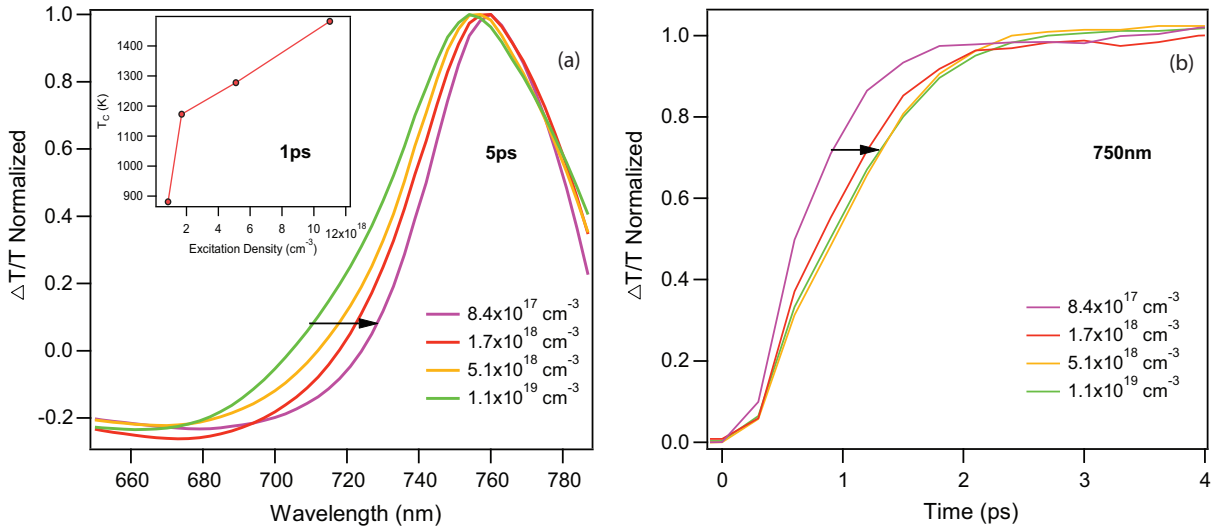

FIG. S3. (a) Normalized (to the PB1 peak) TA spectra near the band-edge as a function of excitation density. Since PB1 originates due to thermalized carriers at the band-edge, high-energy side of the bleach peak corresponds to the exponential tail of the carrier distribution. Therefore narrowing and steepening of the PB peak with decreasing carrier density indicate slow thermalization at elevated excitation densities. Inset shows the carrier temperature (1 ps after photoexcitation) extracted from the high energy tail of PB1 peak using a Boltzmann fit proportional to $E^2 \exp(-E/k_{\mathrm{B}}T_e)$ where E is the photon energy in eV and T_e the carrier temperature and k_{B} the Boltzmann constant. It is clear that at higher excitation densities, cooling rate is slower. (b) Rise time of the PB1 peak increases with excitation density confirming the phonon bottleneck. Arrows indicate evolution of the graphs with the increase of the excitation density.

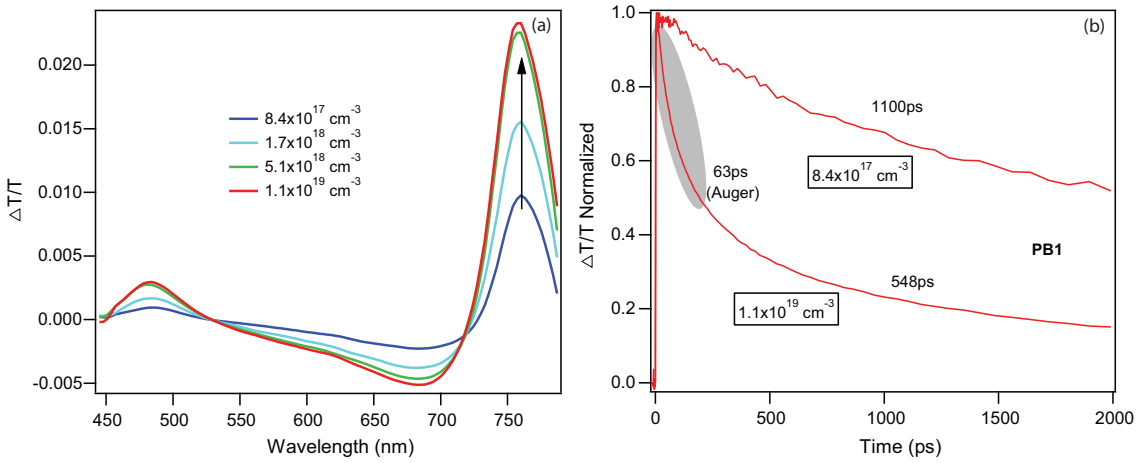

FIG. S4. (a) TA spectra measured as function of excitation density. The PB1 peak does not scale up linearly with excitation density, indicating increased loss of photoexcitations due to Auger type processes. Arrow points towards the increase of the excitation density (b) Dynamics of PB1 (1.6 eV) peak measured as function of the excitation density using a 400 nm pump. At low excitation density (8.4×10^{17} cm^{-3}), the bleach peak decays exponentially with a lifetime of 1100 ps. When the excitation density is increased to 1.1×10^{19} cm^{-3}, the band-edge population follow a bi-exponential decay with a fast initial component of $\sim$ 63 ps, indicative of auger type process. Such many-body processes result from increased carrier-carrier interactions which lead to the transfer of energy and momentum from the recombining electron-hole pair to a third charge carrier.

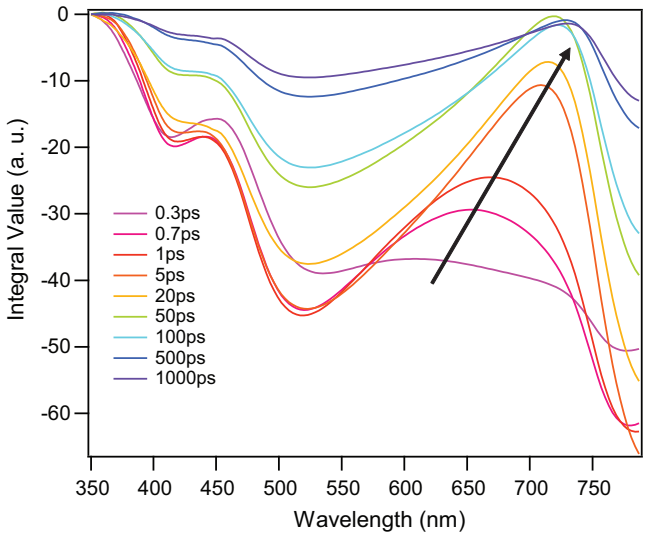

FIG. S5. In relation to the sum rules, Eq. (2) of the main text, we show here the evolution of the partial integrated absorption $\int_{\omega}^{\omega_0} \Delta\alpha \, d\omega$ over a spectral window of frequencies between $\omega = \omega(\lambda)$ and $\omega_0 = \omega(\lambda_0)$ for $\lambda_0 = 350$ nm as a function of λ. Absorption changes $\Delta\alpha$ used here are related to differential transmission spectra as $(-\Delta\alpha \, d) = \ln(1 + \Delta T/T) \cong \Delta T/T$ for small changes in transmittance and neglecting photorefractive variations, with d being the sample thickness. The arrow points in the direction of the increasing delay times. The integral values computed for this window are all negative.

TABLE S1. Lifetime analysis of the transient kinetics measured at the PB peaks shown in Fig. 2 of the main text. While all three PB features as such are long-lived, their dynamics consist of different decay components, ranging from sub-picoseconds to nanoseconds, indicating different relaxation processes. Remarkably, the long components (t_3) of all the PB peaks are similar and are independent of the pump energy confirming the common contribution from thermalized carriers at the fundamental band edge(s). The sub-picosecond dynamics observed with high energy pump arise from the hot carrier relaxation from higher lying valence and conduction bands to the fundamental band-edges. The pump dependence of t_1 and t_2 lifetimes can be attributed to various degrees of auger related relaxation which are sensitive to excitation conditions.

PB peak	550 nm pump			303 nm pump		
λ	t_1 (ps)	t_2 (ps)	t_3 (ps)	t_1 (ps)	t_2 (ps)	t_3 (ps)
750 nm	7±0.3	218±17	1240±46	-	159±12	1189±47
480 nm	5±0.2	185±34	1483±52	0.6±0.03	97±9	1470±118
396 nm	6.3±0.2	134±24	1117±69	0.7±0.07	67±8	1261±57

Macroscopic evaluation of transient transmittance.

We illustrate here the relative effects of the changes in absorption and refraction of the perovskite material on the pump-probe transients. The discussion will be in terms of the frequency-dependent complex dielectric function $\varepsilon(\omega) = \varepsilon'(\omega) + i\varepsilon''(\omega)$ that is used in a standard [1] way to evaluate the transmittance T and reflectance R of our stratified experimental slab.

The spectral behavior of $\varepsilon'(\omega)$ and $\varepsilon''(\omega)$ of $CH_3NH_3PbI_3$ perovskite is shown in Fig. S6(a) as obtained and parameterized in the ellipsometric study [2]. Figure S6(b) displays the calculated T and R of the thin-film structure used in the experiment: light is incident on a layer of PMMA followed by the perovskite film followed by a glass substrate. The first two layers are modeled with the coherent light propagation, while the thicker glass substrate is treated incoherently. PMMA and glass are taken as non-absorbing with a refractive index of 1.5 each and thicknesses of PMMA and $CH_3NH_3PbI_3$ layers are 40 and 60 nm, respectively. One can now vary the dielectric function: $\varepsilon \to \varepsilon + \Delta\varepsilon$, where the variation $\Delta\varepsilon$ is caused by photoexcitation, and calculate the resulting changes in the transmittance: $T \to T + \Delta T$.

In order for $\Delta\varepsilon(\omega)$ to automatically satisfy Kramers-Kronig relations [1, 3], we will use from the outset its spectral representation as follows:

$$\Delta\varepsilon(\omega) = \omega_{\rm pl}^2 \int_0^\infty \frac{f(z)}{z^2 - \omega^2 - i0}\, dz, \tag{1}$$

where

$$f(z) = \frac{2}{\pi\omega_{\rm pl}^2}\, z\, \Delta\varepsilon''(z) \tag{2}$$

is a function describing the spectral changes in the oscillator strengths. As discussed in the main text (see Eq. (2) of the main text), for photoexcitation that does not change the total number of electrons in the system, the total absorptive strength does not change, hence:

$$\int_0^\infty f(z)dz = 0. \tag{3}$$

The conveniently separated factor of $\omega_{\rm pl}^2$ in (1) plays a formal role of the magnitude factor but has also a meaningful physical connotation related to the effective plasma frequency $\omega_{\rm pl}$ of the photoexcited carriers, as introduced in Eq. (3) of the main text. For the Drude-like contribution from the low-frequency *intraband* transitions, one would have then

$$\int_0^{\omega_c} f(z)dz = 1, \tag{4}$$

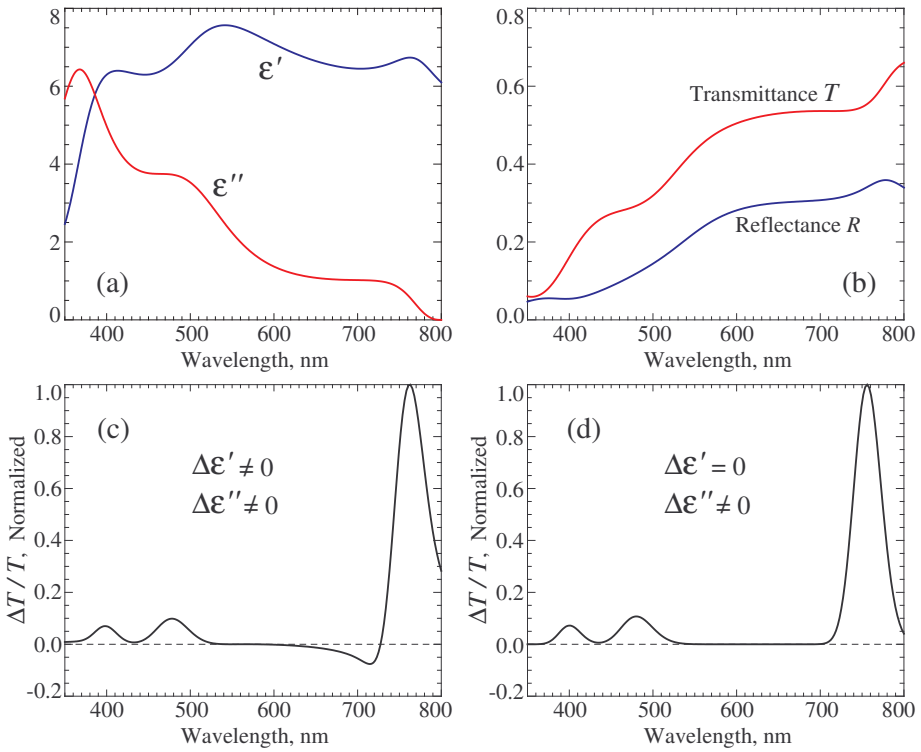

FIG. S6. (a) $\varepsilon'(\omega)$ and $\varepsilon''(\omega)$ of $CH_3NH_3PbI_3$ perovskite shown as a function of the wavelength, per Ref. [2]. (b) The computed linear transmittance T and reflectance R of the structure used in the experiments. (c) The computational result for the transient transmission as derived with the model $\Delta\varepsilon(\omega)$ described in text. (d) The transient transmission that would take place if the changes $\Delta\varepsilon'(\omega)$ were neglected.

where ω_c is well below the fundamental band gap. For the *interband* transitions of our interest here, function $f(z)$ would be correspondingly, Eq. (3), "normalized" as

$$\int_{\omega_c}^{\infty} f(z)dz = -1. \tag{5}$$

Note that with the reduced electron-hole mass $m_r = 0.1m_e$, likely a good order-estimate for perovskites [4], the plasma frequency ω_{pl} would be equal to 0.037, 0.117, and 0.371 eV for the densities n_{eh} of photoexcited electrons (same for holes) equal to 10^{17}, 10^{18}, and 10^{19} cm^{-3}, respectively. In our calculations of the normalized $\Delta T/T$ changes for Fig. S6 we used $\omega_{pl}^2 = 0.01$ eV^2.

While, of course, this macroscopic description can accommodate arbitrary variations $f(\omega)$ of the oscillator strengths, our goal here is to illustrate the results associated exclusively with "pure" interband bleaching variations. We therefore perform calculations with function $f(\omega)$

in Eq. (5) approximately describing experimentally observed PB1, PB2, and PB3 features at long time scales using three Gaussians: (i) centered at $\omega = 1.64$ eV, standard deviation 0.035 eV, and weight 0.67, (ii) centered at $\omega = 2.58$ eV, standard deviation 0.1 eV, and weight 0.2, and (iii) centered at $\omega = 3.1$ eV, standard deviation 0.1 eV, and weight 0.13. The contributions to Eq. (1) for the experimental range of ω from these three optical regions affect both $\Delta\varepsilon'$ and $\Delta\varepsilon''$, while the contribution from the intraband transitions, Eq. (4), adds only to $\Delta\varepsilon'$.

Figure S6(c) displays the normalized $\Delta T/T$ transient resulting from the described model function $f(\omega)$. In order to accentuate the effect of $\Delta\varepsilon'$ on this result, Fig. S6(d) shows what the transient would look like if changes $\Delta\varepsilon'$ in the real part of the dielectric function were neglected. The difference between panels (c) and (d) is quite clear. One particularly notices a negative $\Delta T/T$ feature (looking like PA) in panel (c) slightly above the energy of the PB1 peak, which can thus be characterized as a photorefractive effect due to variations Δn of the refractive index [4]. Comparison of this computed feature with the experimentally observed PA shows, however, that the experimental PA is substantially spectrally broader and larger in magnitude. We therefore conclude that the experimentally observed PA feature between the PB1 and PB2 peaks cannot be understood as just a photorefractive effect.

[1] M. Dressel and G. Grüner, *Electrodynamics of Solids* (Cambridge University Press, Cambridge, 2002).

[2] P. Löper, M. Stuckelberger, B. Niesen, J. Werner, M. Filipič, S. J. Moon, J. H. Yum, M. Topič, S. De Wolf, and C. Ballif, J. Phys. Chem. Lett. **6**, 66 (2015).

[3] Y. Toyozawa, *Optical Processes in Solids* (Cambridge University Press, Cambridge, 2003).

[4] M. B. Price, J. Butkus, T. C. Jellicoe, A. Sadhanala, A. Briane, J. E. Halpert, K. Broch, J. M. Hodgkiss, R. H. Friend, and F. Deschler, Nat. Commun. **6**, 8420 (2015).